Chemistry–A European Journal
Research Article
doi.org/10.1002/chem.202400258
Chemistry Europe
European Chemical Societies Publishing
www.chemeurj.org

Hot Paper

Trifluoromethyl Fluorosulfonate (CF_3OSO_2F) and Trifluoromethoxy Sulfur Pentafluoride (CF_3OSF_5) – Two Gaseous Sulfur(VI) Compounds with Insulating Properties

Paul Golz,[a] Gesa H. Dreyhsig,[a] Holger Pernice,[a] Thomas Drews,[a] Jan H. Nissen,[a] Helmut Beckers,[a] Simon Steinhauer,[a] Anja Wiesner,[a] and Sebastian Riedel*[a]

In this work, we analyzed trifluoromethyl fluorosulfonate (CF_3OSO_2F) and trifluoromethoxy sulfur pentafluoride (CF_3OSF_5) regarding their potential use as dielectrics by investigating some of their intrinsic and extrinsic properties. Both compounds show a higher breakdown voltage than SF_6 with averaged relative breakdown voltages of 1.3 ± 0.2 for CF_3OSO_2F and 1.4 ± 0.2 for CF_3OSF_5 compared to SF_6 with 1.0. Like the dielectric $(CF_3)_2CFCN$, both compounds decompose during the breakdown process. The decomposition products were analyzed by IR spectroscopy and GCIR methods. Furthermore, the molecular structures of both gaseous compounds CF_3OSO_2F and CF_3OSF_5 have been determined by in situ crystallization, and their physical properties were determined as well.

Introduction

Sulfur hexafluoride (SF_6) is one of the most potent greenhouse gases due to its extreme stability in the atmosphere. Most of its emission is human-made and mostly related to its usage as a dielectric.[1,2] In applications like sound insulating glazing, car tires or in sport shoes, SF_6 has been replaced, by air, nitrogen or argon, but it is still used in various industrial processes due to its distinct properties.[3,4] The European Parliament and the Council of the European Union (EU) have ordered the reduction of artificially produced fluorinated gases, particularly SF_6, in an EU regulation. An update in 2022 called for an increased phase out of SF_6 in all new electricity transmission equipment by 2031.[5] However, this phase out proved challenging, as the industrially favored properties of SF_6 are also the reason for its exceptionally long atmospheric lifetime of about 3200 years and the resulting global warming potential (GWP) of around 23900 over a 100 year period.[6–8] The high GWP value is based on the lifetime in the environment and on the ability to absorb IR irradiation. The absorption cross section for fluorinated molecules is often relatively high. Therefore, short lifetimes and low GWP values are becoming important properties in the search for gaseous dielectric media. SF_6 is a colorless, odorless, and non-toxic gas at room temperature, with a high density, a high thermal conductivity, and a low viscosity. These properties enable an effective heat transfer through different media.[3,8,9] Additionally, SF_6 is very temperature stable and shows a remarkably low reactivity towards other chemical compounds and is thus considered to be chemically inert.[10,11]

A valuable approach to replace SF_6 in low (LV) and middle (MV) voltage applications is the use of nitrogen or dry air. Due to their low dielectric strengths, these replacements do not work for high voltage (HV) applications like gas-insulated switchgears (GISs) or gas-insulated transmission lines (GILs). The effective ability of SF_6 to suppress and extinguish electric arcs is based on its high dielectric strength and breakdown voltage, which are directly related to the electronegativity of its elements.[12–14]

Fluorine, the element with the highest electronegativity, forms very stable compounds, and its gaseous compounds often show a high electrical resistance[15] and high breakdown voltage.[12] Consequently, various compounds which are nowadays studied as SF_6-substitutes mostly contain fluorine atoms e.g. CF_3I, C_2F_6, heptafluoroisobutyronitrile ($(CF_3)_2CFCN$, *Novec 4710*), heptafluoroisopropyl trifluoromethyl ketone ($(CF_3)_2CFC(O)CF_3$, *Novec 5110*) and heptafluoroisopropyl pentafluoroethyl ketone ($(CF_3)_2CFC(O)CF_2CF_3$, *Novec 1230*).[3,6] Although these gases provide very high dielectric strengths, some of their properties, such as high boiling points, their decomposition products and possible toxicity, limit their usage on an industrial scale.[16] Furthermore, such PFAS (per- and polyfluorinated alkyl substances) are environmentally problematic due to their unique properties. Therefore, the EU is considering a ban of PFAS with use-specific exemptions and some exclusions where $-CF_3$ or $-CF_2-$ groups are bound to specific heteroatoms.[17]

Accordingly, it is necessary for future dielectrics to be environmentally friendly by enabling a degradation of the compound in the atmosphere into harmless compounds.[3,18] In

[a] P. Golz, G. H. Dreyhsig, H. Pernice, T. Drews, Dr. J. H. Nissen, Dr. H. Beckers, Dr. S. Steinhauer, Dr. A. Wiesner, Prof. Dr. S. Riedel
Fachbereich Biologie, Chemie, Pharmazie
Institut für Chemie und Biochemie – Anorganische Chemie
Freie Universität Berlin
Fabeckstr. 34/36, 14195 Berlin (Germany)
E-mail: s.riedel@fu-berlin.de

Supporting information for this article is available on the WWW under https://doi.org/10.1002/chem.202400258

addition, they must be safe to use, harmless to the used infrastructure and facilitate a well-known industrial handling.[2,19] Furthermore, specific intrinsic and extrinsic properties are required, including basic chemical and physical properties like high dielectric strength (DS), low boiling point and suitable reactivity, including the formation of harmless by-products.[2,13,20] The required high dielectric strength depends on the ability to absorb free electrons and to form anions and thus on the compound-related electron affinity.[12,21,22]

At the outset of this work, we were looking for gaseous compounds with insulating properties that would extend the range of dielectrics and could be considered as substituents for SF_6. Trifluoromethoxy sulfur pentafluoride (CF_3OSF_5) and trifluoromethyl fluorosulfonate (CF_3OSO_2F) are promising candidates as both compounds have high predicted DS values and high adiabatic electron affinities based on quantum chemical evaluations. Furthermore, these compounds show interesting properties such as boiling points of −10 °C[23] (CF_3OSF_5) and −4.2 °C[24] (CF_3OSO_2F) and are accessible from starting materials such as CF_3OF and SF_4[23] or CF_3OF and SO_2,[24] respectively.

Results and Discussion

Synthesis

CF_3OSF_5 and CF_3OSO_2F were prepared by modified literature procedures[23,24] starting from CF_3OF and SF_4 or CF_3OF and SO_2 in a stainless steel autoclave (Scheme 1, a). Reactive species were quenched with soda lime. The gases were obtained in good yields (72% and 69%, respectively) by isothermal distillation. IR spectra recorded in the gas phase of both compounds are consistent with those in the literature.[23,24]

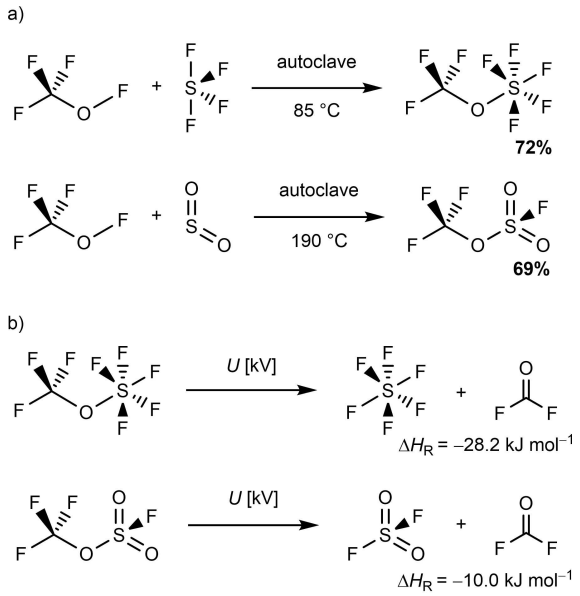

Scheme 1. a) Synthesis of CF_3OSF_5 and CF_3OSO_2F starting from CF_3OF and SF_4 or SO_2, respectively, b) Arc plasma decomposition reactions of CF_3OSO_2F and CF_3OSF_5.

Solid State Structure

Both substances have low melting points (−156.5 °C for CF_3OSO_2F and −161.6 °C for CF_3OSF_5, Table 1). Crystals suitable for X-ray analysis were obtained by in situ crystallization. Their recorded molecular structures are in accordance with DFT-calculations. In CF_3OSO_2F (Figure 1, top), both the sulfur and the carbon atoms show a slightly distorted tetrahedral coordination environment with a geometry index of $\tau_4 = 0.96$ for carbon and $\tau_4 = 0.89$ for sulfur.[25] Both moieties are connected via O1 with a C1–O1–S1 bond angle of 122.0(2)° and C1–O1 and O1–S1 bond distances of 141.7(4) and 157.3(2) pm. The distortion of the sulfur-based tetrahedron might be caused by the repulsion of the lone pairs of F1 with those of O2 and O3. This assumption is corroborated by the slightly longer S1–O2, S1–O3 and S1–F1 bond distances of 139.9(3), 139.0(3), and 152.7(2) pm, respectively, compared to the molecular structure of solid sulfuryl fluoride (SO_2F_2) with 138.6(2) for the S–O bonds and 151.4(2) pm for the S–F bonds.[26] In the structurally related molecule $CF_3OSO_2CF_3$, the two terminal S–O bonds and the bridging S–O bond are with distances of 141.1(3), 141.4(4) and 160.7(3) pm, respectively, longer than in CF_3OSO_2F. On the other hand, the C1–O1 bond of CF_3OSO_2F is with 141.7(4) pm longer than the C–O bond in $CF_3OSO_2CF_3$ with 139.9(5) pm. Additionally, the bond angle O2–S1–O3 of 124.2(2)° shows similar values to the corresponding angles in SO_2F_2 and $CF_3OSO_2CF_3$ with 124.6(1)°

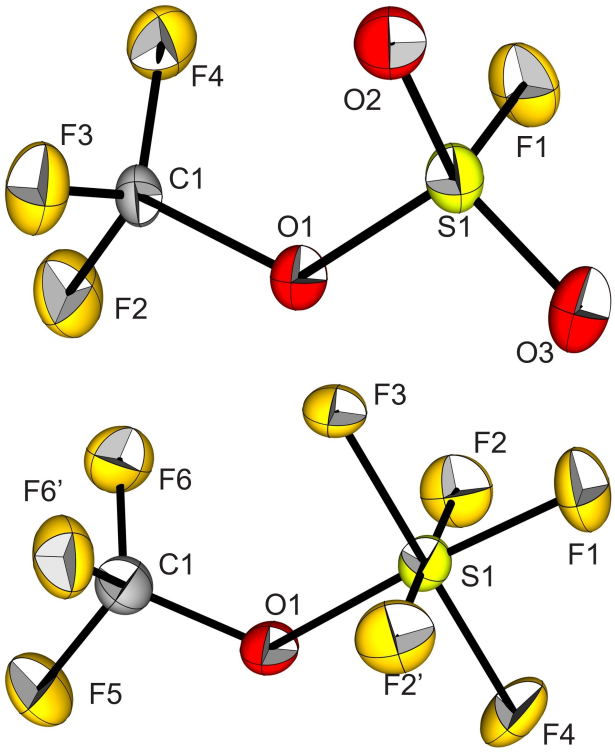

Figure 1. Molecular structures in the solid state of CF_3OSO_2F (top) and CF_3OSF_5 (bottom). Thermal ellipsoids are set at 50% probability. Selected bond lengths [pm] and angles [°] of CF_3OSO_2F: 141.7(4) (C1–O1), 157.3(2) (O1–S1), 139.9(3) (S1–O2), 139.0(3) (S1–O3); 152.7(2) (S1–F1), 121.9(2) (C1–O1–S1), 124.2(2) (O2–S1–O3), 106.8(2) (O2–S1–F1). Selected bond lengths [pm] and angles [°] of CF_3OSF_5: 137.2(3) (C1–O1), 163.8(2) (O1–S1), 125.1(2) (C1–O1–S1).

and 123.5(2)°, respectively. This is also the case for the O2–S1–F1 bond angle of 106.8(2)° when compared to this angle in SO_2F_2 with 107.6(1)°[26] and for the C1–O1–S1 bond angle of 121.9(2)° compared to $CF_3OSO_2CF_3$ with a value of 122.0(3)°.[27]

The molecular structure of CF_3OSF_5 (Figure 1, bottom) shows a carbon-based tetrahedron ($\tau_4 = 0.95$) and a sulfur-based octahedron, both connected by O1. The C1–O1–S1 bond angle of 125.1(2)° is widened, the O1–S1 bond distance of 163.8(2) pm longer and the C1–O1 bond of 137.2(3) pm shorter than that in CF_3OSO_2F. However, the C–F bonds of the CF_3 group and the S–F bonds show almost the same lengths in both compounds. Additionally, these S–F bond distances are similar to those in SF_6.[28]

Gas Phase Data

The vapor pressures of CF_3OSO_2F and CF_3OSF_5 were measured in two temperature ranges by using different setups. The *Antoine*-parameters *A*, *B* and *C* (see Table S7) were determined using a multiple linear regression of the measured vapor pressure curves. The parameters are valid for the *Antoine*-equation using *p* [bara] and *T* [K].[29] The first range was chosen in a temperature window around the boiling points known from the literature, −4.2 °C[24] (CF_3OSO_2F) and −10 °C[23] (CF_3OSF_5). The measurements carried out led to a re-evaluation of the boiling points at −5.5 °C (CF_3OSO_2F) and −10.5 °C (CF_3OSF_5). In comparison, SF_6 has a sublimation point of −63.8 °C[10] and is therefore used as dielectric even at low temperatures. CF_3OSO_2F and CF_3OSF_5, like the *Novec* compounds, are more limited to higher temperatures. Using a setup for the determination of critical parameters (see SI, Figure S11), we measured the vapor pressures in a larger temperature range from low temperatures to temperatures above the critical points of the substances.

We were able to determine the critical points due to the visible change from the two-phase system (gas and liquid phase) into a supercritical fluid. The critical points were reached at $T_{crit} = 110.7 \pm 0.7$ °C, and $p_{crit} = 28.7 \pm 0.1$ bara for CF_3OSO_2F and at $T_{crit} = 123.5 \pm 0.8$ °C, and $p_{crit} = 32.2 \pm 0.1$ bara for CF_3OSF_5 (Table 1). Knowing the critical point of a substance, its *van der Waals*-constants a and b were estimated (see Table S4) using the *van der Waals*-equation.[29]

The gas densities ρ_{gas} were determined to be 7.1 ± 0.1 kg m^{-3} (CF_3OSO_2F) and 8.9 ± 0.1 kg m^{-3} (CF_3OSF_5) at 26.0 °C and a pressure of 1013 mbar (Table 1). These gas phase densities are higher than those of SF_6 (6.0 ± 0.1 kg m^{-3}).

Table 1. Melting point ($T_{m.p.}$), boiling point ($T_{b.p.}$), gas phase density at 26 °C (ρ_{gas}) and critical parameters (T_{crit} and p_{crit}) of CF_3OSO_2F and CF_3OSF_5

	CF_3OSO_2F	CF_3OSF_5
$T_{m.p.}$ [°C]	−116.4 ± 2.0	−142.0 ± 2.0
$T_{b.p.}$ [°C]	−5.5 ± 0.5	−10.5 ± 0.5
ρ_{gas}(26.0 °C) [kg m^{-3}]	7.1 ± 0.1	8.9 ± 0.1
T_{crit} [°C]	110.7 ± 0.7	123.5 ± 0.8
p_{crit} [bara]	28.7 ± 0.1	32.2 ± 0.1

Quantum Chemistry

Quantum chemical calculations were performed to support the experimental data. Geometry optimizations of the structures on the B3LYP–D3/def2-TZVP level of theory provided consistent structures to those obtained by X-ray analysis and enabled the assignments of the gas-phase IR bands (see Table S1). Both optimized structures were used for a NBO analysis. Furthermore, evaluations at the BP86-D3/def2-QZVPP level of theory were used to predict DS values by the method of Rabie *et al.*[30] Obtained by DFT calculations of anionic, neutral, and cationic species, values for the electric dipole moment (μ), the average static electronic polarizability (α), the adiabatic ionization energy (ε_i) and the number of electrons (N_e), showing high relative DS of 1.7 and 2.1 for CF_3OSO_2F and CF_3OSF_5, respectively, compared to SF_6 (1.0). In addition, higher adiabatic electron affinity values (ε_a) of −2.9 eV (CF_3OSF_5) and −2.4 eV (CF_3OSO_2F) compared to SF_6 (−2.1 eV) were also obtained.

Dielectric Strength and Decomposition Behavior

Based on calculated predictions, high DS values are expected for both compounds. One method to analyze the DS of a compound, is the determination of its breakdown voltage U_{BD}. Therefore, we developed a simplified method to determine the U_{BD} of different gases. The setup was realized by using a 250 mL flask with a *Young* valve and two electrodes with an adjustable distance facing each other. After filling the flask with a certain pressure of the gas, a voltage (AC, 230 V–10.5 kV, 50 Hz) was applied and increased, until an arc became visible between the electrodes (Figure 2). Measurements of the breakdown voltages U_{BD} as a function of the electrode spacing (Figure 3) were carried out with the gaseous dielectrics at an initial pressure of 0.1 bara and electrode distances between 0.2 and 1.0 cm. The U_{BD} of CF_3OSF_5 and CF_3OSO_2F showed better results compared to SF_6, demonstrating higher electrical resistances and thus higher dielectric strengths. The averaged relative insulation

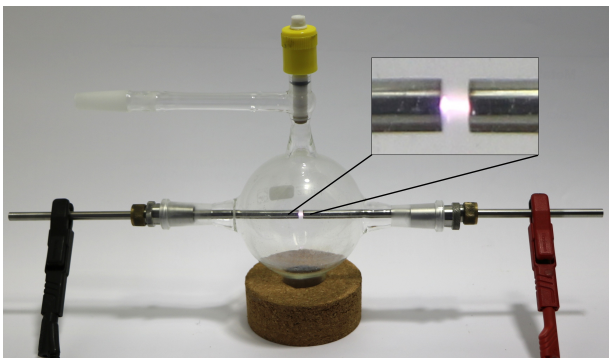

Figure 2. Experimental setup for the determination of dielectric properties during an arc event.

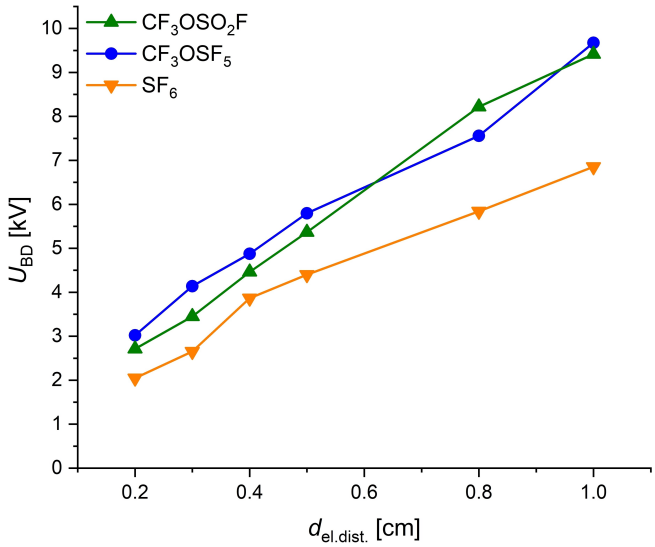

Figure 3. Breakdown voltages U_{BD} [kV] as a function of the distance between the electrodes $d_{el.dist.}$ [cm] used for CF_3OSO_2F (▲), CF_3OSF_5 (●) and SF_6 (▼) at an initial pressure of $p_i = 0.1$ bara.

strength of CF_3OSF_5 (1.4 ± 0.2) and CF_3OSO_2F (1.3 ± 0.2) are lower than the predicted ones. Nevertheless, the values are higher than for SF_6, which is set to 1 by definition. The higher DS values are in accordance with the higher gas densities compared to SF_6, as the electrical resistance of a gas is roughly proportional to its density.[31] Potential SF_6 substitutes with higher insulation characteristics than SF_6, such as $(CF_3)_2CFCN$ (2.2) and $(CF_3)_2CFC(O)CF_3$ (2.0), already exist.[3] However, potential SF_6 substitutes must also provide adequate decomposition characteristics.

As already mentioned, electric arcs can appear during switching operations of high voltages. These are high energy events where the dielectric medium gets ionized and temperatures around 10,000 K are possible.[16] Under these extreme conditions, SF_6 splits into several sulfur fluoride species like $[SF_5]^•$ or SF_4 and mainly $F^•$ radicals inside the arc plasma. Extinguishing this arc will lead to a rapid, thermodynamically favored recombination of these molecules to SF_6. To a lesser extent, $[SF_5]^•$ radicals can recombine to the highly toxic S_2F_{10}, and in the presence of H_2O or O_2, other toxic compounds like SF_4, SO_2F_2, or HF can be formed. Due to the favored recombination to SF_6, the overall decomposition is rather low.[3,16] For other dielectrics such as $(CF_3)_2CFCN$, the decomposition is much more favored. A mixture of $(CF_3)_2CFCN$ (53 %) in air (47 %) shows a degradation of the nitrile of 61.7 % after 200 breakdown processes with a duration of ~10 ms each, while only a small amount (1.6 %) of SF_6 is decomposed under the same conditions.[32] This can be explained by a lower recombination rate of the more complex nitrile and the thermodynamically favored formation of other reaction products. Some of the decomposition products like CF_4, C_2F_6, or C_2N_2 have a high GWP, while several are also highly toxic like CF_3CN, C_4F_8, and HF. This leads to a drastically increased acute toxicity with a lethal concentration (LC_{50}) of the nitrile mixture that is around 1100 times lower than that of pure SF_6 after 200 breakdown processes.[32]

To analyze the decomposition behavior of CF_3OSO_2F and CF_3OSF_5, experiments were conducted at their breakdown voltages. The gas was exposed to a stable arc over a period of 10 s at an initial pressure of $p_i = 0.1$ bara, which corresponds to 1000 breakdown processes with a duration of 10 ms each. IR spectra of the gas phase after the arc revealed the partial decomposition of CF_3OSF_5 and CF_3OSO_2F. The undecomposed portion φ of the dielectric determined after discharge depends on the electrode distance (Figure 4). At larger distances between the electrodes, φ decreases in breakdown processes, which corresponds to *Paschen*'s law.[21,33] While the decomposition of CF_3OSF_5 with $\varphi = 19\,\%$ is already well advanced at electrode distances of ≥ 0.8 cm, the decomposition of CF_3OSO_2F is less favored, as the undecomposed portion was $\varphi = 42\,\%$ at the largest electrode spacing of 1.0 cm used (Figure 4).

IR spectra of the gas mixture after the electrical breakdown in gaseous CF_3OSF_5 revealed CF_2O and SF_6 as main decomposition products (Scheme 1, b). The formation of SF_6 during the decomposition process significantly limits the suitability of this compound as an SF_6 substitute. CF_3OSO_2F shows similar properties in terms of boiling point and a good DS value as CF_3OSF_5, but the tendency to form SF_6 during arcing events should be lower due to the lower fluorine but higher oxygen content. IR spectra of the gas mixture formed after the electrical breakdown revealed CF_2O and SO_2F_2 as the main decomposition products (Scheme 1, b). Both compounds are toxic while SO_2F_2 is also a greenhouse gas. However, as rather reactive species, these products can be hydrolyzed, especially with basic media like soda lime. CF_3OSO_2F itself is quite stable towards hydrolysis and was only partially hydrolyzed after contact to 5 M NaOH at 100 °C for 39 h, as reported by Wayne et al.[24] This gives CF_3OSO_2F a clear advantage over other SF_6 substitutes currently

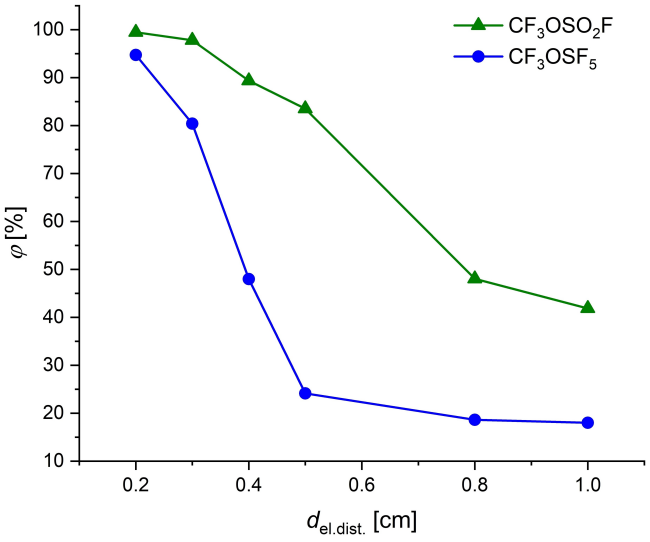

Figure 4. Undecomposed amount of dielectric φ [%] after arc-exposition as a function of the electrode distance $d_{el.dist.}$ [cm] for CF_3OSO_2F (▲) and CF_3OSF_5 (●).

in use, whose decomposition products can mostly not be hydrolyzed.

Decomposition Pathways

CF_3OSF_5 and CF_3OSO_2F decompose in a similar way during arcing events into two main species each (cf. Scheme 1, b). For CF_3OSO_2F, this can mainly be explained by a labile S–O bond. NBO analysis shows that the lowest unoccupied molecular orbital can be regarded as the σ*-bond orbital between the sulfur atom and the bridging oxygen atom (Figure 5, left). The formation of $[CF_3O]^\bullet$ and $[SO_2F]^\bullet$ radicals seems to be feasible. These can either recombine, or the $[CF_3O]^\bullet$ radical eliminates an $F^\bullet$ radical which then reacts with the $[SO_2F]^\bullet$ radical under formation of SO_2F_2 (Scheme 2, a). Transferring this tentative mechanism to CF_3OSF_5 would also explain the decomposition products SF_6 and CF_2O. However, NBO analysis of CF_3OSF_5 reveals a LUMO mainly localized at the σ*-bond orbital between the sulfur atom and the apical fluorine atom (Figure 5, right). This suggests a mechanism in which the dissociation into $F^\bullet$ and $[CF_3OSF_4]^\bullet$ radicals is favored. $[CF_3OSF_4]^\bullet$ could then decay into $[CF_3O]^\bullet$ radicals and SF_4. The reaction between these two species could lead to the formation of SF_6 and CF_2O (Scheme 2, b).

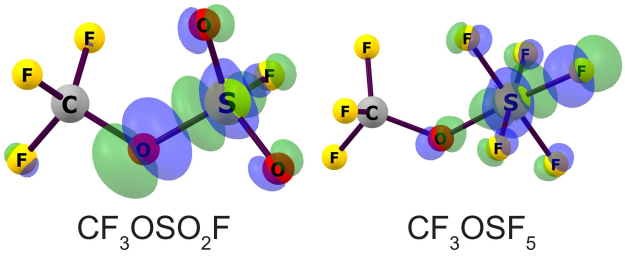

Figure 5. Quantum chemical calculations of the lowest unoccupied natural bond orbitals (NBO) at B3LYP–D3/def2-TZVP level of theory of CF_3OSO_2F (left) and CF_3OSF_5 (right).

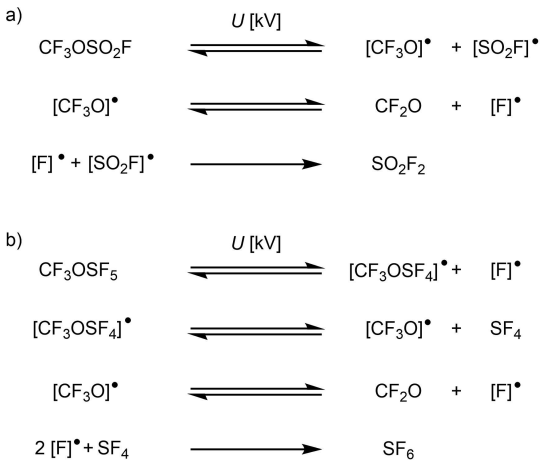

Scheme 2. Tentative decomposition reaction pathways of a) CF_3OSO_2F and b) CF_3OSF_5.

Quantum chemical calculations at the B3LYP–D3/def2-TZVP level of theory provide reaction enthalpies of $-10.0\ kJ\,mol^{-1}$ and $-28.2\ kJ\,mol^{-1}$ for these decomposition pathways of CF_3OSO_2F and CF_3OSF_5, respectively (cf. Scheme 1). Although both reaction sequences are slightly exothermic, the activation barrier for their decomposition appears to be high. However, it can be overcome in an arc with high energy.

Conclusions

Trifluoromethyl fluorosulfonate (CF_3OSO_2F) and trifluoromethoxy sulfur pentafluoride (CF_3OSF_5) were (re–)evaluated with regard to their intrinsic and extrinsic properties in the solid, liquid and gas phase. We were able to determine the molecular structures in the solid state for both CF_3OSO_2F (b.p.: −5.5 °C) and CF_3OSF_5 (b.p.: −10.5 °C). Measurements of the liquid and the gas phase led to the determination of their critical parameters (T_{crit} and p_{crit}), their *van der Waals*-constants a and b, and their *Antoine*-parameters *A*, *B*, and *C*. With averaged relative breakdown voltages of 1.3 (CF_3OSO_2F) and 1.4 (CF_3OSF_5), both substances show better insulation properties than SF_6 and are comparable to $(CF_3)_2CFCN$.[16] All three substances (CF_3OSO_2F, CF_3OSF_5, and $(CF_3)_2CFCN$) show higher decomposition rates than SF_6 during arcing events. CF_3OSF_5 decomposes into SF_6 which affects its potential use as an SF_6 replacement. In contrast, CF_3OSO_2F is more stable and decomposes into the hydrolysable compounds CF_2O and SO_2F_2 during arcing events. Due to the short perfluorinated chains, CF_3OSO_2F and CF_3OSF_5 can be considered as degradable materials and are exempt from the planned PFAS ban. For their potential use as dielectrics, further studies will be conducted to evaluate their toxicity, GWP, or their compatibility with materials.

Experimental Section

Reagents and Analytical Techniques

All gases were handled using standard Schlenk techniques and oil pump vacuum up to 10^{-3} mbar. Commercially available SO_2 (Linde), SF_4 (abcr), SF_6 (Linde) and R134a (Linde) were used without further purification. CF_3OF was prepared according to a literature procedure.[34]

X-ray diffraction measurements were performed on a Bruker D8 Venture diffractometer with a CMOS area detector using CuKα radiation. Single crystals were obtained using in situ crystallization and selectively melting of the substances in capillaries installed on the diffractometer in a cooled nitrogen stream at −148 °C. The structures were solved using the ShelXT structure solution program using intrinsic phasing and refined with the ShelXL refining package using least-squares minimization by using OLEX2. For graphical representations, the programs Diamond 4 and POV-Ray 3.7 were used. IR spectra were recorded with eight scans and a resolution of 4 cm^{-1} using a Bruker Vector 22 FTIR spectrometer or a Thermo Fisher Scientific Nicolet™ iS50 FTIR spectrometer in combination with a Thermo Fisher Scientific TRACE™ 1310 GC-Analyzer gas chromatograph. The programs OPUS 7.5 and OMNIC 48 were used for the evaluation of the recorded spectra, and Origin 2022 for the graphical representation. NMR spectra were recorded

using a JEOL 400 MHz ECZR or ECS spectrometer and all chemical shifts are referenced using the Ξ values given in the *IUPAC* recommendations of 2008 and the ^{2}H signal of the deuterated solvent as internal reference.[35] For external locking, acetone-d_6 was flame sealed in a glass capillary and the lock oscillator frequency was adjusted to give $\delta(^{1}H) = 7.26$ ppm for a $CHCl_3$ sample locked on the capillary. For strongly coupled spin systems all chemical shifts and coupling constants are reported as simulated in gNMR.[36] MestReNova 14.2 was used for processing the spectra and for their graphical representation. Quantum chemical calculations were conducted using program Orca 5.0.3[37] on the HPC system provided by the ZEDAT (Freie Universität Berlin, Curta).[38] The B3LYP[39] or BP86[40] functionals (with D3BJ[41]) were used with the basis sets def2-TZVP or def2-QZVPP.[42] For the NBO analysis the software extension NBO 7.0.4[43] was used.

General Synthesis: Reactions were carried out in a 500 mL stainless steel autoclave (Model IV, Carl Roth) of 740 mL (gas) capacity equipped with a 100 bar bursting disk. The autoclave was tempered by a silicon oil bath and an electric magnetic stirrer (*IKA® RCT standard safety control*, IKA-Werke, Staufen im Breisgau, Germany) for stirring and heating. After the reaction the autoclave was cooled to room temperature and the gaseous material was released through an U-shaped stainless-steel tube filled with soda lime into a dry ice cooling trap. To prevent the product from decomposition the temperature of the soda lime was kept below 60 °C. The raw material was then condensed into a liquid nitrogen cooled trap by applying a vacuum (1×10^{-3} mbar). The products were obtained by fractional isothermal distillation and stored in stainless steel vessels.

CF_3OSF_5

54 g (0.5 mol, 1 eq.) SF_4 and 53 g (0.51 mol, 1.02 eq.) CF_3OF were condensed into the autoclave and after warming to room temperature it was heated to 85 °C for 48 h. The product (76.1 g, 0.36 mmol, 72 %) was obtained as colorless gas via distillation. $T_{b.p.}$ −10.5 °C. **^{19}F NMR** (377 MHz, neat, external [D_6]acetone, 21 °C): δ (ppm) = 66.1 (m, 4F_B, $^{2}J(^{19}F_B, ^{19}F_A) = 153.1$ Hz, $^{4}J(^{19}F_B, ^{19}F_{CF}) = 10.0$ Hz), 58.9 (m, 1F_A, $^{2}J(^{19}F_A, ^{19}F_B) = 153.1$ Hz, $^{4}J(^{19}F_A, ^{19}F_{CF}) = 1.4$ Hz), −59.5 (dquint, 3F, OCF_3, $^{4}J(^{19}F_A, ^{19}F_{CF}) = 1.4$ Hz, $^{4}J(^{19}F_B, ^{19}F_{CF}) = 10.0$ Hz, $^{1}J(^{19}F_{CF}, ^{13}C) = 266$ Hz). **^{13}C NMR** (101 MHz, neat, external [D_6]acetone, 21 °C): δ (ppm) = 119.6 (qquint, $^{1}J(^{13}C, ^{19}F_{CF}) = 266$ Hz, $^{3}J(^{13}C, ^{19}F) = 2.1$ Hz). **^{17}O NMR** (54 MHz, neat, external [D_6]acetone, 21 °C): δ (ppm) = 212 (s). **^{33}S NMR** (31 MHz, neat, external [D_6]acetone, 21 °C): δ (ppm) = −182 (sext, $^{1}J(^{33}S, ^{19}F) = 250$ Hz).

CF_3OSO_2F

4.6 g (72 mmol, 1 eq.) SF_4 and 13.8 g (133 mmol, 1.85 eq.) CF_3OF were condensed into the autoclave and after warming to room temperature it was heated to 190 °C for 48 h. The product (8.4 g, 50 mmol, 69 %) was obtained as a colorless gas via distillation. $T_{b.p.}$ −5.5 °C **^{19}F NMR** (377 MHz, neat, external [D_6]acetone, 21 °C): δ (ppm) = 45.0 (q, 1F_S, $^{4}J(^{19}F, ^{19}F) = 6.7$ Hz), −58.4 (d, 3F_C, $^{4}J(^{19}F, ^{19}F) = 6.7$ Hz, $^{1}J(^{19}F, ^{13}C) = 273$ Hz). **^{13}C NMR** (101 MHz, neat, external [D_6]acetone, 21 °C): δ (ppm) = 118.8 (q, $^{1}J(^{13}C, ^{19}F) = 273$ Hz). **^{17}O NMR** (54 MHz, neat, external [D_6]acetone, 21 °C): δ (ppm) = 191 (s, OCF_3), 164 (d, 2O, SO_2F $^{2}J(^{17}O, ^{19}F) = 35$ Hz).

Determination of Intrinsic Properties

Densities were analyzed by weighing the mass of the gas in a defined volume depending on its pressure and temperature. Critical points were determined optically by observing an opalescence between the coexisting phases of the substance using a pressure-resistant fused quartz tube inside a temperature-adjustable autoclave with quartz windows. The same setup was used for measurements of vapor pressure curves above 1 bara while measurements at lower pressures were performed using a classical Schlenk tube. Melting points were determined by placing the sample, in a sealed glass ampoule, in a beaker containing liquid nitrogen and liquified propane which was slowly heated so that the substance liquified evenly.

Determination of Extrinsic Properties

Electrical discharge properties were determined by measuring the breakdown voltages of the substance of interest at an initial pressure of $p_i = 0.1$ bara and at different distances between two electrodes. Insulation strengths of the investigated gases relative to SF_6 were calculated as a function of the electrode distance. Decomposition products of CF_3OSO_2F and CF_3OSF_5 were analyzed by IR spectroscopy after exposure to an electrical arc for a defined period of ten seconds. In addition to measuring IR spectra of the product mixtures immediately after the electrical discharge, these mixtures were also analyzed with a GCIR system by separating them into their individual components and characterizing them using IR spectroscopy.

Deposition Numbers 2308232 (for CF_3OSO_2F) and 2308230 (for CF_3OSF_5) contain the supplementary crystallographic data for this paper. These data are provided free of charge by the joint Cambridge Crystallographic Data Centre and Fachinformationszentrum Karlsruhe Access Structures service.

Supporting Information

The authors have cited additional references within the Supporting Information.[44]

Acknowledgements

The authors would like to thank the HPC Service of ZEDAT, Freie Universität Berlin, for computing time and gratefully acknowledge the assistance of the Core Facility BioSupraMol supported by the DFG. P.G. and G.D. thank Nils Wehowsky for help designing the TOC graphic. Open Access funding enabled and organized by Projekt DEAL.

Conflict of Interests

This work was carried out partly in cooperation with Solvay Fluor GmbH, Hannover. At the time this work was carried out, H. Pernice was employed by Solvay Fluor GmbH. This collaboration resulted in a patent,[45] in which the Solvay Fluor GmbH, FU-Berlin, as well as the authors S. Riedel, H. Beckers, S. Steinhauer, and H. Pernice hold shares. All other authors declare no conflict of interest.

Data Availability Statement

The data that support the findings of this study are available from the corresponding author upon reasonable request.

Keywords: trifluoromethoxylated sulfur(VI) fluorides · SF_6 substitutes · dielectric properties · decomposition pathways · solid state structures

[1] a) L. Stuart, J. Luterbacher, L. Paterson, R. Devillier, S. Castonguay, *United in Science 2022. A multi-organization high-level compilation of the most recent science related to climate change, impacts and responses*, **2022**; b) L. K. Gohar, K. P. Shine, *Weather* **2007**, *62*, 307; c) P. Widger, A. Haddad, *Energies* **2018**, *11*, 2037.
[2] L. G. Christophorou, J. K. Olthoff, R. J. van Brunt, *IEEE Electr. Insul. Mag.* **1997**, *13*, 20.
[3] S. Tian, X. Zhang, Y. Cressault, J. Hu, B. Wang, S. Xiao, Y. Li, N. Kabbaj, *AIP Adv.* **2020**, *10*, 050702.
[4] a) J. Harnisch, W. Schwarz, *Costs and the impact on emissions of potential regulatory framework for reducing emissions of hydrofluorocarbons, perfluorocarbons and sulphur hexafluoride*, **2003**; b) P. G. Simmonds, M. Rigby, A. J. Manning, S. Park, K. M. Stanley, A. McCulloch, S. Henne, F. Graziosi, M. Maione, J. Arduini, S. Reimann, M. K. Vollmer, J. Mühle, S. O'Doherty, D. Young, P. B. Krummel, P. J. Fraser, R. F. Weiss, P. K. Salameh, C. M. Harth, M.-K. Park, H. Park, T. Arnold, C. S. Rennick, L. P. Steele, B. Mitrevski, R. H. J. Wang, R. G. Prinn, *Atmos. Chem. Phys.* **2020**, *20*, 7271.
[5] a) *European Commission - Press release Green Deal: Phasing down fluorinated greenhouse gases and ozone depleting substances*, Brussels, **2022**; b) Regulation (EU) No 517/2014 on fluorinated greenhouse gases and repealing Regulation (EC) No 842/2006, *Off. J. Eur. Communities: Legis.* **2014**, *L150*, 195.
[6] J. Owens, A. Xiao, J. Bonk, M. DeLorme, A. Zhang, *Energies* **2021**, *14*, 5051.
[7] M. Melinda, M. Manning, D. Qin, S. Solomon, K. Averyt, M. Tignor, H. L. Miller, Jr., Z. Chen, *IPCC, 2007: Climate Change 2007. The Physical Science Basis*, Cambridge (UK) and New York (USA), **2007**.
[8] T. F. Stocker, D. Qin, G.-K. Plattner, M. Tignor, S. K. Allen, J. Boschung, A. Nauels, Y. Xia, V. Bex and P. M. Midgley, *IPCC, 2013: Climate Change 2013. The Physical Science Basis*, Cambridge (UK) and New York (USA), **2013**.
[9] A. A. Lindley, A. McCulloch, *J. Fluorine Chem.* **2005**, *126*, 1457.
[10] A. F. Holleman, N. Wiberg, *Lehrbuch der Anorganischen Chemie*, de Gruyter, Berlin, **2007**.
[11] a) E. Riedel, C. Janiak, *Anorganische Chemie*, de Gruyter, Berlin, Boston, **2015**; b) P. W. Atkins, T. L. Overton, J. P. Rourke, M. T. Weller, F. A. Armstrong, *Shriver & Atkins' inorganic chemistry*, Oxford Univ. Press, Oxford, **2010**.
[12] W. M. Leeds, T. E. Browne, A. P. Strom, *Trans. Am. Inst. Electr. Eng. Part 3* **1957**, *76*, 906.
[13] L. G. Christophorou, *Electron-Molecule Interactions and Their Applications. Volume 2*, Elsevier Science, Burlington, **1984**.
[14] E. E. Kunhardt, L. H. Luessen (Eds.) *NATO Advanced Science Institutes Series, 89a*, Springer, Boston, MA, **1983**.
[15] a) A. Haupt (Ed.) *Organic and Inorganic Fluorine Chemistry*, de Gruyter, Berlin, Boston, **2021**; b) P. R. Howard, *Proc. Inst. Electr. Eng., Part A UK* **1957**, *104*, 139.
[16] X. Li, H. Zhao, A. B. Murphy, *J. Phys. D* **2018**, *51*, 153001.
[17] BAuA (DE), RIVM (NL) KEM (SE), NEA (NO), DEPA (DK), *Annex XV Restriction Report Per- and Polyfluoroalkyl Substances (PFAS)*, Helsinki, **2023**.
[18] M. Rabie, C. M. Franck, *Environ. Sci. Technol.* **2018**, *52*, 369.
[19] C. M. Franck, J. Engelbrecht, M. Muratović, P. Pietrzak, P. Simka, *B&H Electrical Engineering* **2021**, *15*, 19.
[20] R. C. Tolman, *Phys. Rev.* **1917**, *9*, 237.
[21] M. S. Naidu, V. Kamaraju, *High voltage engineering*, McGraw-Hill, New York, **1996**.
[22] A. Chachereau, A. Hösl, C. M. Franck, *J. Phys. D* **2018**, *51*, 495201.
[23] G. Pass, H. L. Roberts, *Inorg. Chem.* **1963**, *2*, 1016.
[24] W. P. van Meter, G. H. Cady, *J. Am. Chem. Soc.* **1960**, *82*, 6005.
[25] L. Yang, D. R. Powell, R. P. Houser, *Dalton Trans.* **2007**, 955.
[26] D. Mootz, A. Merschenz-Quack, *Acta Crystallogr. Sect. C* **1988**, *44*, 924.
[27] T. Knuplez, L. N. Schneider, T. Preitschopf, Y. K. J. Bejaoui, L. Zapf, N. Schopper, K. A. M. Maibom, J. A. P. Sprenger, F. Gehrke, S. Lorenzen, R. Graf, R. Bertermann, I. Fischer, N. V. Ignat'ev, M. Finze, *Chem. Eur. J.* **2023**, *29*, e202302701.
[28] L. S. Bartell, S. K. Doun, *J. Mol. Struct.* **1978**, *43*, 245.
[29] P. W. Atkins, J. de Paula, *Atkins' Physical chemistry*, Oxford University Press, Oxford, New York, **2006**.
[30] M. Rabie, D. A. Dahl, S. M. A. Donald, M. Reiher, C. M. Franck, *IEEE Trans. Dielectr. Electr. Insul.* **2013**, *20*, 856.
[31] L. G. Christophorou, J. K. Olthoff, *Gaseous Dielectrics VIII*, Springer, Boston, MA, **1998**.
[32] F. Ye, X. Zhang, Y. Li, Q. Wan, J.-M. Bauchire, D. Hong, S. Xiao, J. Tang, *High Volt.* **2022**, *7*, 856.
[33] L. Ledernez, F. Olcaytug, G. Urban, *Contrib. Plasma Phys.* **2012**, *52*, 276.
[34] R. C. Kennedy, G. H. Cady, *J. Fluorine Chem.* **1973**, *3*, 41.
[35] R. K. Harris, E. D. Becker, S. M. Cabral de Menezes, P. Granger, R. E. Hoffman, K. W. Zilm, *Pure Appl. Chem.* **2008**, *80*, 59.
[36] Adept Scientific, *gNMR V 5.0*, **2005**.
[37] F. Neese, *WIREs Comput. Mol. Sci.* **2012**, *2*, 73.
[38] L. Bennett, B. Melchers, B. Proppe, *Curta: A General-purpose High-Performance Computer at ZEDAT, Freie Universität Berlin*, **2020**, Freie Universität Berlin, DOI:10.17169/refurbium-26754.
[39] A. D. Becke, *J. Chem. Phys.* **1993**, *98*, 5648.
[40] A. D. Becke, *Phys. Rev. A* **1988**, *38*, 3098.
[41] a) S. Grimme, S. Ehrlich, L. Goerigk, *J. Comput. Chem.* **2011**, *32*, 1456; b) S. Grimme, J. Antony, S. Ehrlich, H. Krieg, *J. Chem. Phys.* **2010**, *132*, 154104.
[42] F. Weigend, R. Ahlrichs, *Phys. Chem. Chem. Phys.* **2005**, *7*, 3297.
[43] E. D. Glendening, J. K. Badenhoop, A. E. Reed, J. E. Carpenter, J. A. Bohmann, C. M. Morales, P. Karafiloglou, C. R. Landis, F. Weinhold, *NBO 7.0*, Theoretical Chemistry Institute, University of Wisconsin, Madison, WI, **2018**.
[44] a) D. Atack, W. G. Schneider, *J. Phys. Chem.* **1951**, *55*, 532; b) A. Diefenbacher, M. Türk, *Fluid Phase Equilib.* **2001**, *182*, 121; c) K. Morofuji, K. Fujii, M. Uematsu, K. Watanabe, *Int. J. Thermophys.* **1986**, *7*, 17.
[45] J. Fabre, F. Hardinghaus, H. Pernice, S. Hasenstab-Riedel, H. Beckers, S. Steinhauer, T. Schlöder PCT Int. Appl. (2017), WO 2017093510 A1.

Manuscript received: January 20, 2024
Accepted manuscript online: February 8, 2024
Version of record online: February 27, 2024